Lasers in Manufacturing Conference 2017

Experimental and theoretical analysis of thermo-optical effects in protective window for selective laser melting

Tobias Bonhoff[a,*], Maximilian Schniedenharn[b], Jochen Stollenwerk[a,b], Peter Loosen[a,b]

[a]*RWTH Aachen University, Chair for Technology of Optical Systems, Steinbachstr. 15, 52074 Aachen, Germany*
[b]*Fraunhofer Institute for Laser Technology, Steinbachstr. 15, 52074 Aachen, Germany*

Abstract

The objective of this work is to study thermo-optical effects in protective windows for selective laser melting. Therefore, an interface to couple finite element analysis and wave-optical analysis is used. The laser beam caustic is analyzed for three different protective window materials, fused silica, N-BK7, and N-FK51A. The impact of contamination of the window by metal plume is investigated experimentally and theoretically. The simulations predict the highest focus shift for a contaminated fused silica window whereas N-FK51A has nearly no impact on the beam caustic due to its athermalized behavior. The experimental results reveal that an increasing contamination is accompanied by an increasing focus shift and a decreasing beam quality.

Keywords: selective laser melting; thermal lensing; protective window; finite elemente analysis

1. Introduction

Selective Laser Melting (SLM) of metal parts is frequently suffering from thermo-optical effects, especially those in the protective window that separates the optical elements from the processing chamber. Absorption of laser energy in the bulk material, in the AR-coatings, and, in particular, contamination by metal plume causes heating of the protective window. The inhomogeneous temperature distribution in the window causes a locally varying refractive index and surface deformations. These altered optical properties

* Corresponding author. Tel.: +49-241-8906-379; fax: +49-241-8906-497.
E-mail address: tobias.bonhoff@tos.rwth-aachen.de.

will induce a focus shift as well as higher order aberrations. As a consequence, the SLM process will be disturbed.

The coupling of finite element analysis (FEA) and ray-tracing is a common approach for analyzing thermally induced effects in optical systems such as protective windows. Different approaches for approximating discrete finite element data (temperature and deformation) and for transferring the results to optical ray-tracing programs have been established during the last years (Genberg et al., 2002, Mazzolli et al., Gatej et al., 2012). However, all these approaches are suffering from the fundamental limitation that ray-tracing is not valid in the focal region where diffraction has to be considered. Although most ray-tracing engines provide a basic wave-optical functionality, for example to compute the intensity distribution in a certain image plane, an analysis of a laser beam caustic is not possible. In addition, the field distribution of a laser beam source, for instance a higher-order Gaussian beam, cannot be defined.

In order to overcome these limitations, we introduce a novel interface to couple FEA and wave-optical analyses using VirtualLab Fusion. Section 2 discusses how the discrete FE-data for the temperature distribution and for the surface deformations are approximated, and how the interface to VirtualLab is realized. The coupling of FEA and wave-optics is applied in Section 3 to analyze the laser beam caustic of an SLM machine with different materials as protective window. Finally, the influence of different degrees of the window's contamination are analyzed and compared to experimental measurements of the focus shift in Section 4.

2. Coupling of finite element analysis and wave-optical analysis

The coupling of FEA and wave optical analysis contains of four steps. Firstly, the thermo-mechanical analysis is performed using ANSYS® Workbench. It is based on the optical model in order to define the thermal loads properly. Secondly, the discrete FE-data for the temperature distribution and for the surface deformations are approximated using special algorithms (Section 2.1). Then, the continuously differentiable functions for the refractive index profile and for the surface deformations are transferred via a Dynamic Link Library (DLL) to programmable surfaces and medium in VirtualLab (Section 2.2). Finally, the wave-optical analysis is performed and the laser beam caustic is analyzed (Section 2.3). Fig. 1 gives an overview of this procedure.

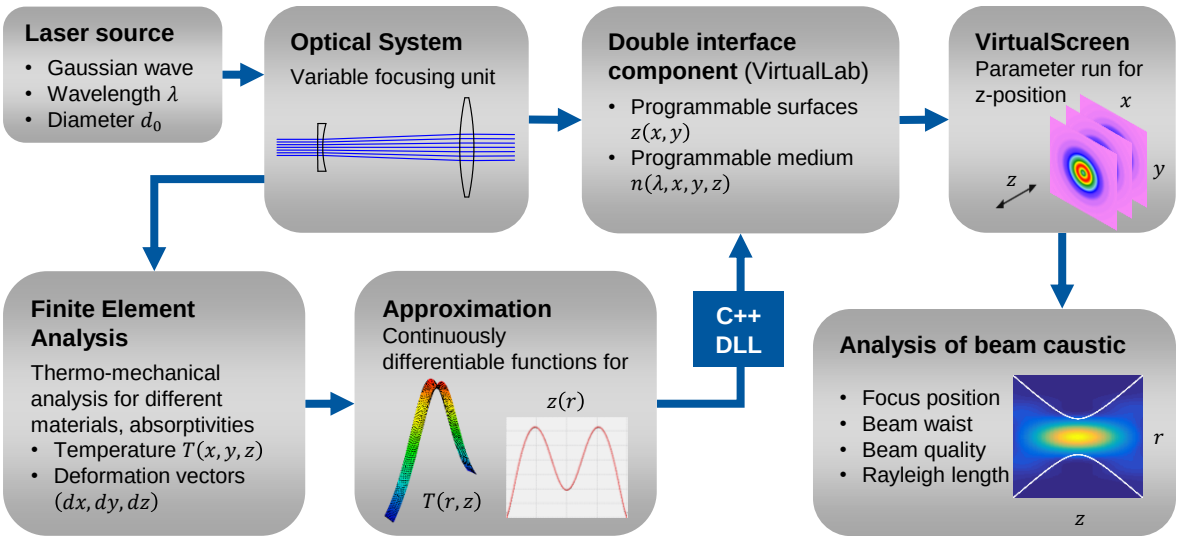

Fig. 1. Visualization of the coupling of FEA and wave-optical analysis.

2.1. Approximation of the finite element data

VirtualLab exhibits (in version 6.2.1.15) a feature to import external data of a refractive index profile or the shape of a surface. But these data have to be defined on an equidistant grid. Since FE meshes are usually non-equidistant, the data have to be either transferred to an equidistant grid or directly transferred into continuously differentiable functions. We take the second approach because suitable algorithms for approximating non-equidistant FE-data have already been developed and are used for the coupling of FEA and ray-tracing (Gatej et al., 2012, Bonhoff et al., 2015).

The utilized weighted least squares approximation algorithm is highly flexible. It applies polynomials functions onto locally restricted areas. The local areas are adaptively refined in order to reach a user-defined error threshold. The global function, either for the temperature or for the surface deformation, is assembled by combing the local functions using distinct weighting functions. More details on the algorithm can be found in the work of Gatej et al., 2012.

2.2. Coupling using a Dynamic Link Library

In VirtualLab, a so-called double interface component is used to model the protective window. Thereby, the front and back surface are set as programmable surfaces and the bulk material as programmable medium. The user can apply own code to define either the surface shape or the refractive index profile. We use a C++ DLL to link an external data file, which contains the information on the approximated refractive index profile and the approximated surfaces, to the code in VirtualLab.

For the programmable surfaces, the DLL returns both, the z-position of the surface at a given position (x, y) and the local gradients $\mathrm{d}z/\mathrm{d}x$ and $\mathrm{d}z/\mathrm{d}y$. For the programmable medium, the DLL returns the refractive index $n(\lambda, x, y, z)$ for a certain wavelength λ at a given position in the medium. VirtualLab then computes the local gradients numerically. In case that the material data are available, a formula for the refractive index change in dependence on wavelength and on temperature increase ΔT,

$$\frac{\mathrm{d}n}{\mathrm{d}T} = \frac{n^2(\lambda,T_0)-1}{2n(\lambda,T_0)}\left(D_0 + 2D_1\Delta T + 3D_2\Delta T^2 + \frac{E_0 + 2E_1\Delta T}{\lambda^2 - \lambda_{tk}^2} \right), \quad (1)$$

is applied (Schott, 2016). Eq. (1) is integrated in order to obtain the refractive index $n(\lambda, \Delta T)$. Especially for large temperature increases, this model is to be preferred to a constant thermo-optical coefficient $\mathrm{d}n/\mathrm{d}T$.

2.3. Wave-optical analysis

In order to analyze the laser beam caustic in dependence on the thermal load, which the protective window exhibits, the field distribution is computed in numerous subsequent planes using a so-called parameter run in VirtualLab. For the propagation from the protective window into the focal region, the combined spectrum of plane waves/ Fresnel operator is used. The parameter run yields the 3-dimensional field distribution in the focal region.

Since the analyzed optical system (c.f. Section 3) is rotationally symmetric, only a cross-section in radial direction of the squared field amplitude $A^2(r,z)$ is exported for further analyses. For each z-plane, the beam radius $w(z)$ is computed according to the method of 2nd moment (ISO 11146). Then, a caustic fit is performed to obtain the waist location z_0, the waist radius w_0, and the beam quality M^2.

The presented approach for a thermo-optical analysis in VirtualLab is currently limited to paraxial systems and plane substrates, exhibiting only small surface deformations. The reason for this are limitations of the double interface component, which is the only component that enables the user to define a refractive index profile $n(x,y,z)$. The applied split-step beam propagation method is only applicable for media with small refractive index changes and paraxial conditions (Wyrowski, 2016, Thylen, Yevick, 1982). In addition, refraction at the surfaces of the double interface component is treated using the thin element approximation which assumes paraxial conditions, too.

However, for the performed analyses in Section 3, the above mentioned conditions are fulfilled. The numerical aperture is about 0.01 and the deformations of the protective window are in the range of a few micrometer.

3. Simulations

In the following, the thermo-optical behavior of three different materials as protective window for SLM is investigated. In addition to fused silica, which is commonly used for protective windows, the Schott glasses N-BK7 and N-FK51A are analyzed. Furthermore, the influence of an increased absorptivity, caused by the contamination of the window, is examined.

3.1. Setup and material parameters

The setup is visualized in Fig. 2. The laser beam is focused into the processing plane with a variable focusing unit that enables a variable shift of the focus in dependence on the scanning angle. The laser scanner is omitted in the model because the central position is analyzed only. The protective window is 150 mm in diameter and 2 m thick. The incident laser beam features a Gaussian shape and its diameter on the window is 10.3 mm. The focal positon is located about 476 mm (BFL) below the protective window in case of a clean window and 400 W laser power.

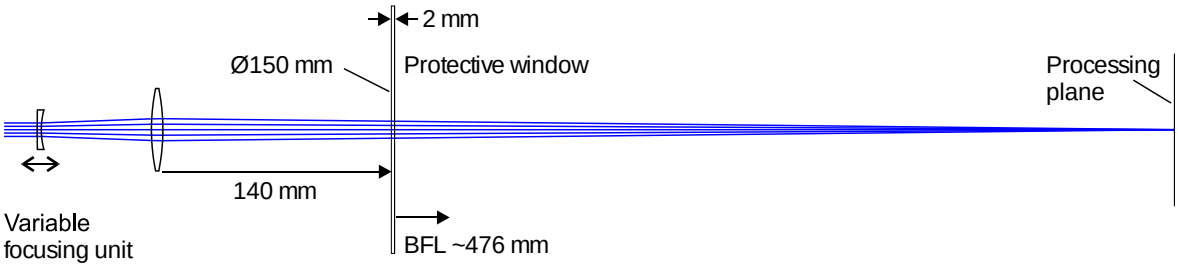

Fig. 2. Sketch of the optical setup for the simulation. The laser scanner is omitted in the model.

The relevant material parameters for the simulations are listed in Table 1. According to Koechner, 1970, the ratio of the refractive powers induced by the temperature dependent refractive index profile and the thermal surface deformation can be estimated by the factor

$$\beta = \frac{(n-1)\alpha_{th}}{\mathrm{d}n/\mathrm{d}T}. \qquad (2)$$

Fused silica features a comparably large thermo-optic coefficient $\mathrm{d}n/\mathrm{d}T$ but a small thermal expansion coefficient α_{th}. Thus, the influence of the refractive index change dominates and β = 2.7%. On the contrary, thermal surface deformation predominates for the standard glass N-BK7 because β = 382%. For the glass N-FK51A, both thermal effects contribute nearly the same amount to the refractive power (β = −97%). Consequently, N-FK51A is almost self-compensating. Materials with this characteristic are also called athermalized.

For the two glasses, the parameters for the temperature dependent thermo-optic coefficient are available (Schott, 2015) and, thus, Eq. (1) is used. For fused silica, only a constant thermo-optic coefficient $\mathrm{d}n/\mathrm{d}T$ of $9.6 \cdot 10^{-6}$/K is available for a temperature range from 20 to 25°C. This might cause inaccuracies for temperature increases >25°C, which is the case for contaminated windows as thermography measurements indicate.

Fused silica features the smallest absorption coefficient in the bulk material, whereas N-BK7 and N-FK51A absorb approximately 60 and 120 times more laser energy in the bulk. For the clean protective windows, an absorptivity in the anti-reflection coatings of 0.01% is assumed. This assumption is based on own measurements of the absorptivity of comparable optical elements by photothermal common-path interferometry. The influence of the window's contamination by the deposition of metal plume is investigated by increasing the absorptivity of the back surface stepwise from 0.1% up to 0.5%, because the additional absorptivity within the experiments is in the sub-percent range (c.f. Section 4.1).

Table 1. Relevant material parameters of fused silica (Corning, 2008) and the Schott glasses N-BK7 and N-FK51A (Schott, 2015).

Material of protective window	Fused silica	N-BK7	N-FK51A
Refractive index n(1060 nm)	1.4497	1.5067	1.4761
Thermo-optic coefficient $\mathrm{d}n/\mathrm{d}T$ [10^{-6}/K]	9.6	1.1	−7.3
Coefficient of thermal expansion α_{th} [10^{-6}/K]	0.57	8.3	14.8
Thermal conductivity κ [W/(m K)]	1.38	1.12	0.76
Factor for self-compensation β [%]	2.7	382	−97
Absorption coefficient bulk material [%/cm]	0.002	0.12	0.24
Absorptivity AR-coating [%]	0.01	0.01	0.01
Additional absorptivity caused by contamination of the protective window's backside [%]	0.1 up to 0.5	0.1 up to 0.5	0.1 up to 0.5

3.2. Beam caustic and focus shift

The results of the wave-optical analysis in VirtualLab are analyzed as described in Section 2.3. The normalized intensity distribution $I(r,z)$ in the focal region is depicted in Fig. 3 for a protective window made of fused silica. The fitted beam caustic is visualized as white lines. The back focal length z_0 (with respect to the window's back surface) is 476.1 mm for the clean window, and 454.5 mm for an additional absorptivity of 0.5%. In addition to the focus shift of −21.6 mm (corresponding to −4.8 z_R) at 400 W, the waist radius w_0 increases about 30% and, thus, the beam quality decreases. The intensity distribution in the shifted focus plane is similar to that in the original plane; only a small ring structure around the central Gaussian distribution becomes visible.

When comparing the fitted beam caustics for the three materials and a clean and a contaminated protective window (Fig. 4), the following arises. The focus shift induced by the contamination is in case of fused silica slightly bigger than for N-BK7 (−21.6 mm compared to −18.6 mm), although fused silica features the smaller intrinsic absorption coefficient (c.f. Table 1). This can be explained by the large thermo-optical coefficient of fused silica. This material property is disadvantageous when the material heats up caused by an additional absorptivity. As expected based on the factor for self-compensation, N-FK51A induces the smallest focus shift with −1.3 mm (corresponding to −0.29 z_R) at 400 W laser power. In addition, the waist radius and the beam quality stay unaltered. This agrees with the characteristic of an athermalized glass.

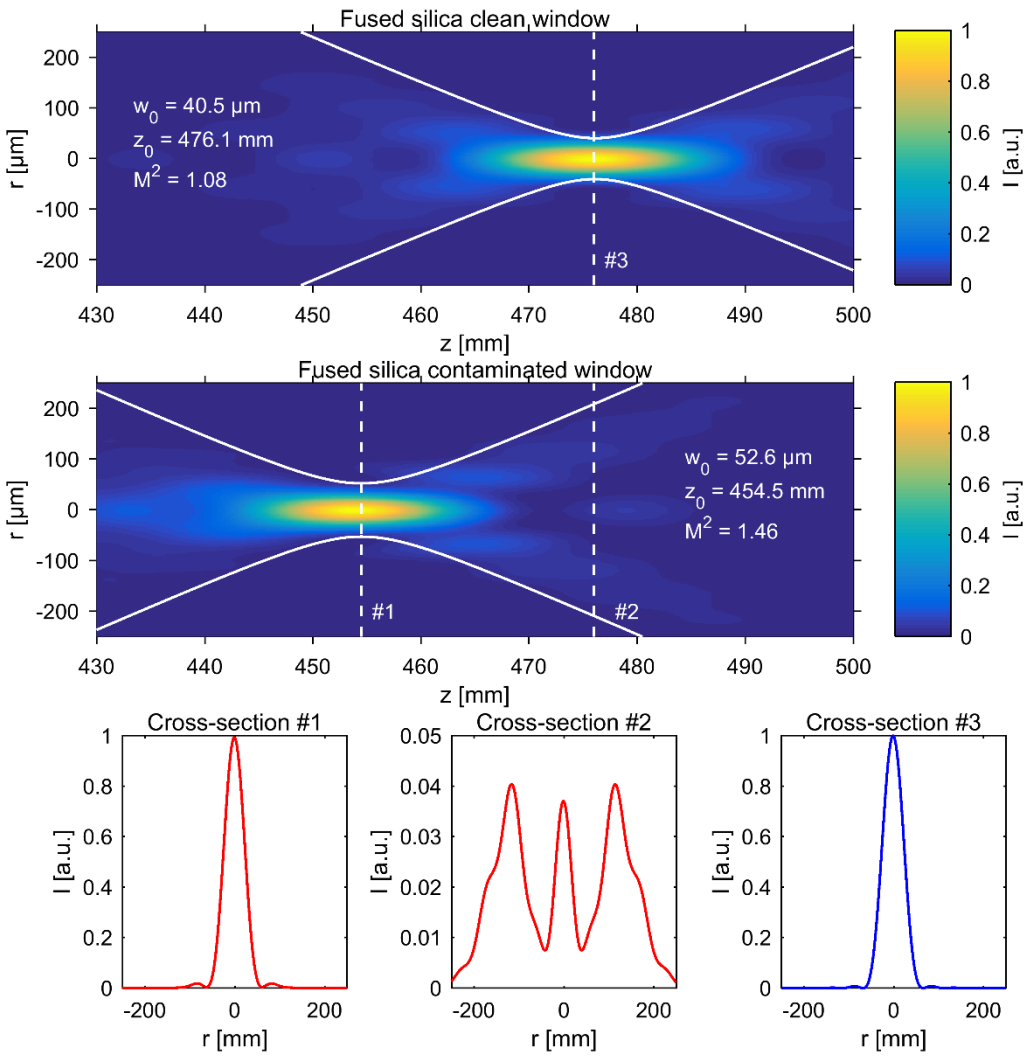

Fig. 3. Normalized intensity distribution in the focal region and fitted beam caustic (white curves) for a clean protective window made of fused silica (top) and an additional absorptivity of 0.5% on the back surface caused by metal plume (middle). The graphs on bottom show cross-sections of the intensity distributions in the three indicated z-planes. The laser power is 400 W.

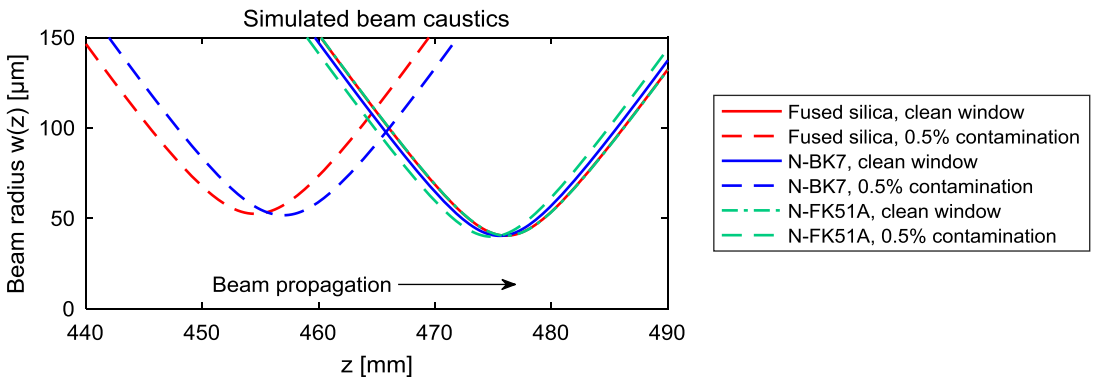

Fig. 4. Simulated laser beam caustics for the three different materials. Comparison of a clean protective window (solid lines) and an additional absorptivity of 0.5% on the back surface caused by metal plume (dashed lines). The laser power is always 400 W.

4. Experimental results

In the following, the experimental results for a clean and a contaminated protective window made of fused silica are presented and compared to the performed simulations.

4.1. Experimental setup

For the experiments, an SLM machine is used that contains a variable focusing unit, a laser scanner, and a protective window as shown in Fig. 2. The utilized fiber laser features a fundamental Gaussian beam. The laser beam caustic is analyzed in thermal equilibrium for the central scan position and a certain state of the protective window's contamination. The intensity distributions are measured in 10 up to 20 subsequent planes in the direction of beam propagation using a CCD-camera. Then, the beam radii are computed based on the method of 2^{nd} moment and a caustic fit is performed.

The series of experiments starts with a clean protective window made of fused silica. Then, the SLM process is started but with a reduced volume flow of the cross jet below the protective window in order to accelerate the contamination process. After a volume of 39.6 cm^3 is generated, the process is stopped and the beam caustic is analyzed again. This procedure is repeated another two times after an accumulated volume of 71.6 and 104.8 cm^3 is generated. In the end, the protective window is cleaned using isopropanol and the beam caustic is measured in order to compare it to the initial one. The window's absorptivity has not been measured since the window cannot be removed during the series of experiments. However, an upper threshold for the absorptivity of 1% can be estimated based on the measurement of the transmitted laser power.

4.2. Results and comparison

The measured laser beam caustics are depicted in Fig. 5 and directly compared to the simulative results. Both are referenced to the focus position for the clean window.

The increased contamination of the window (contamination 1-3 in Fig. 5) leads to a focus shift of −22 mm up to −30 mm. In addition, the waist radius increases from 35 µm to 53 µm. The window exhibits the highest increase in absorptivity caused by contamination during the first period with a reduced volume flow of the cross jet. Within the simulations, an additional absorptivity of 0.5% leads to similar results for the focus shift and the increase of beam waist as in the experiments. After cleaning the protective window, the focus

position nearly equals those at the beginning of the series of experiments. This is a clear evidence that the window's contamination increases the absorptivity and, thus, induces thermally effects.

In Fig. 5, the intensity distributions in four selected focus planes are depicted, too. In the experimental results, a stronger ring around the central Gaussian distribution is visible than in the simulations. However, in both cases the amount of laser energy contained in this ring increases with an increasing contamination of the protective window. This might be traced back to thermally-induced aberrations.

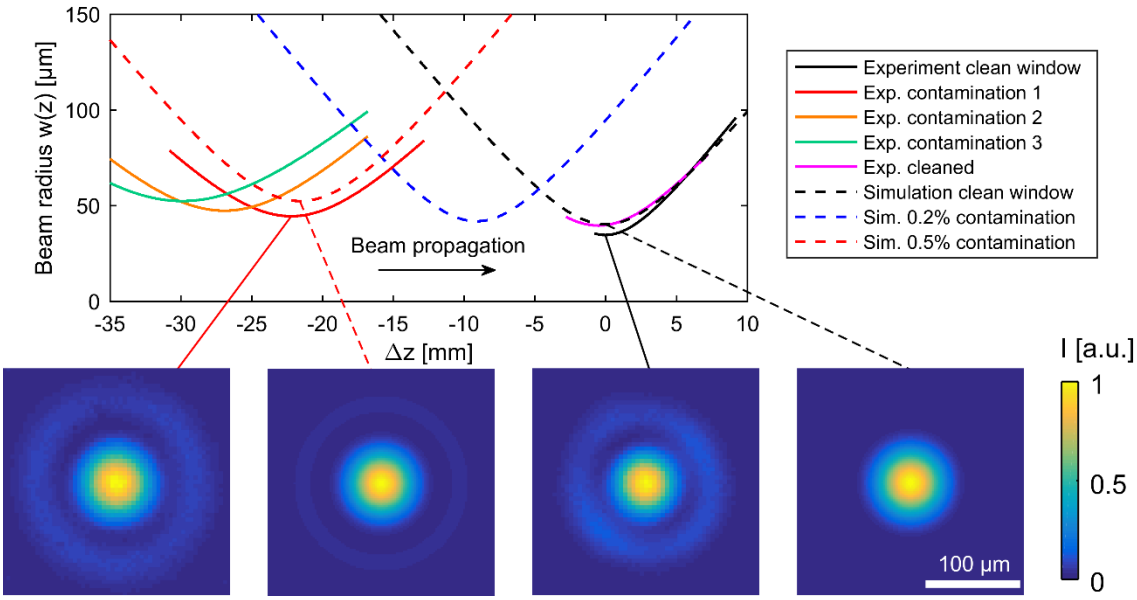

Fig. 5. Measured and simulated laser beam caustics for the protective window made of fused silica (top). Intensity distributions in four selected focus planes (bottom). The laser power is always 400 W.

5. Conclusion

Thermally induced effects in protective windows for SLM strongly depend on the state of contamination. The deposition of metal plume increases the window's absorptivity and causes a focus shift and a decrease of the beam quality. Both effects reduce the component quality of the SLM parts. In contrast, the loss of laser power caused by contamination is circumstantial for the component quality.

An interface to couple finite element analyses and wave-optical analyses in VirtualLab Fusion is presented. It enables a precise analysis of the laser beam caustic for different materials as protective window and variant contaminations. The simulations predict in case of an additional absorptivity, for example caused by metal plume, that windows made of fused silica induce a larger focus shift than those made of N-FK7. In contrast, the focus shift induced by athermalized glasses such as N-FK51A is negligible with about −0.3 Rayleigh lengths. Within the experiments, it is shown that fused silica protective windows induce strong focus shifts and an increase of the beam waist if it is contaminated by metal plume.

The authors plan to extend the experimental analysis to protective windows made of other glasses than fused silica. In the field of modeling, work on the extension to non-paraxial systems and curved substrates such as lenses is planned. In addition, the transient thermal behavior of the protective window will be analyzed in order to obtain more practice-oriented values for the focus shift and aberrations during the highly dynamic SLM process.

Acknowledgements

This work was supported by the German Research Foundation (DFG) within the project “Experimental and theoretical studies of thermally induced aberrations in optical systems for laser material processing” (LO 640/11-1).

References

Bonhoff, T., Büsing, L., Stollenwerk, J., Loosen, P., 2015. Modeling of optical aberrations due to thermal deformation using finite element analysis and ray-tracing, Proc. of SPIE 9626, p. 96261.

Corning Inc., 2008. HPFS® Fused Silica Standard Grade. Semiconductor Optics.

Gatej, A., Wasselowski, J., Loosen, P., 2012. Using adaptive weighted least squares approximation for coupling thermal and optical simulation, Applied Optics 51, pp. 6718–6725.

Genberg, V. L., Michels, G. J., Doyle, K. B., 2002. Making FEA Results Useful in Optical Analysis, Proc. of SPIE 4769, pp. 24–33.

Koechner, W.. 1970. Thermal Lensing in a Nd:YAG Rod, Appl. Opt. 9, pp. 2548–2553.

Mazzoli, A., Saint-Georges, P., Orban, A., Ruess, J.-S., Loicq, J., Barbier, C., Stockman, Y., Georges, M., Nachtergaele, P., Paquay, S., de Vincenzo, P., 2011. Experimental validation of opto-thermo-elastic modeling in OOFELIE multiphysics, Proc. of SPIE 8167, p. 81671.

Schott AG, 2015. Optical Glass. Data Sheets.

Schott AG, 2016. Technical Information TIE-19, version July 2016. Temperature Coefficient of the Refractive Index.

Thylen, L., Yevick, D., 1982. Beam propagation method in anisotropic media, Applied Optics, 21(15), p.2751–2754.

Wyrowski VirtualLab, User’s Manual, July 2016.